Non-scanning CARS microscopy using wide-field geometry

I.Toytman[1], K.Cohn[1], T. Smith[1], D. Simanovskii[1]and D. Palanker[1,2]
[1]Hansen Experimental Physics Laboratory, Stanford University, 445 Via Palou, Stanford, CA 94305
[2]Department of Ophthalmology, Stanford University School of Medicine, 300 Pasteur Drive, Stanford, CA 94305

ABSTRACT

We report a wide-field Coherent Anti-Stokes Raman Scattering (CARS) microscopy technique based on non-phase-matching illumination and imaging systems. This technique is based on a non-collinear sample illumination by broad laser beams and recording image of sample at anti-Stokes wavelength using full-frame image detector. An amplified Ti:Sapphire laser and an Optical Parametric Amplifier (OPA) provided picosecond pump and Stokes beams with energies sufficient for CARS generation in an area of 100 μm in diameter. The whole field of view of the microscope was illuminated simultaneously by the pump and Stokes beams, and CARS signal was recorded onto a cooled CCD, with resolution determined by the microscope objective. Several illumination schemes and several types of thin sample preparations have been explored. We demonstrated that CARS image of a 100x100 μm sample can be recorded with submicrometer spatial resolution using just a few laser pulses of microJoule energies.

Keywords: Coherent anti-Stokes Raman scattering, Microscopy, Wide-field, Fast imaging, Chemically selective imaging, Multiphoton microscopy, Scanning microscopy

1. INTRODUCTION

Low natural optical contrast of biological cells and tissues often necessitates staining of the samples with various chromophores and fluorescent markers. However, exogenous staining is limited in applications to living cells due to its effect on cellular metabolism. Thus optical techniques for imaging of living cells with intrinsic chemical contrast and high spatial resolution are of great interest. Mid-IR absorption microscopy can provide chemical selectivity, but it has limited spatial resolution due to long (3-10 μm) wavelengths, and is difficult to apply in aqueous media due to high water absorption. Raman microscopy overcomes these problems by generating chemically-selective signals in the visible range, therefore providing resolution on the order of 1 micrometer. However, small cross section of spontaneous Raman scattering limits the sensitivity of the method and requires high laser power and long exposures. Furthermore, spontaneous Raman spectroscopy at visible wavelengths suffers from fluorescent background that reduces the contrast of acquired images. These problems are circumvented in CARS microscopy, which is based on a nonlinear light generation in a four-wave mixing process [1]. Utilization of visible and near IR (less than 1 μm) wavelengths makes spatial resolution comparable to that of a conventional visible light microscope and allows for imaging of aqueous samples. Since anti-Stokes component has a wavelength shorter than the pump wavelength, CARS signal is free of fluorescent background. In addition, CARS signal can be much stronger than spontaneous Raman scattering due to coherent nature of this emission process determined by constructive interference of signals from individual molecular vibrations over the interaction length [2].

After theoretical description of the process by Maker and Terhune [3] and first implementation of CARS microscope by Duncan et al [4] numerous studies were performed to increase the image brightness and resolution as well as the acquisition speed [5-7]. Starting from Zumbush et al. [8] most of the CARS systems have been based on scanning approach, in which two collinearly focused beams produce the signal in a small focal volume. In this geometry the interaction length, over which CARS signal is generated is on the order of Rayleigh range Z_0. For Gaussian beam with waist W_0 corresponding Rayleigh length is defined by

$$Z_0 = \frac{\pi \cdot W_0^2}{\lambda}$$

In order to increase spatial resolution very tight focusing with large numerical aperture (NA) objectives is commonly used. In this approach the focal spot size is comparable to the wavelength of the beam. With the pump and Stokes beams focused to a spot with waist diameter $W_0 \sim 1$ μm the Rayleigh length Z_0 is on the order of several micrometers. The axial and lateral extent of the focal zone defines the spatial resolution of scanning method. Relatively short interaction length resulting from tight focusing provides high axial resolution close to the depth of field of a conventional microscope objective, thus allowing for 3-dimensional imaging using layer-by-layer scanning of the sample.

We have explored a wide-field approach to CARS microscopy that would allow for simultaneous image acquisition similarly to a conventional microscope with a focal plane array detector. Since the signals from all points of the sample are recorded simultaneously, there are no strict requirements to pulse-to-pulse stability of the lasers. However, a homogeneous illumination pattern is required to ensure similar conditions for CARS generation over the sample area.

First attempts to implement a wide-field system were made by Heinrich et al. [9]. In their illumination geometry phase-matching conditions were satisfied within a sample. In our opinion, this resulted in a high level of background signal generated in a bulk, which masked chemically specific CARS signal from the small-scale samples features.

Our approach is based on non-collinear non-phase-matching sample illumination geometry that would result in a very low signal generation in the bulk. After refraction, or scattering of the laser beams on a small object, some portion of the pump and Stokes beams will be deflected in a way that satisfies phase-matching condition. Therefore CARS signal can be generated only inside the scattering objects and in their immediate vicinity. In this respect proposed illumination scheme is similar to a dark-field illumination. Intensity of the generated CARS signal will depend on optical properties of the scattering or refracting objects within the sample, as well as on their chemical composition. If the scattering center exhibits Raman-active vibrational modes, CARS signal from that particular object will be strongly enhanced, highlighting its chemical composition. Since this approach to CARS imaging relies on low scattering in the bulk of the sample, it is best suitable for optically thin samples.

2. EXPERIMENTAL SETUP

2.1 Illumination scheme

We tested the proposed technique using an experimental setup built around an inverted microscope (Axiovert 35, Carl Zeiss), diagrammatically shown in Figure 1. The pump and Stokes beams were generated using Ti:Sapphire regenerative amplifier (Regen) and Optical Parametric Amplifier (OPA) system (Spectra-Physics, CA). 794 nm radiation from the Regen was used as a pump beam, and a frequency doubled signal from the OPA, tunable in the range from 1017 – 1055 nm was used as a Stokes beam.

Pump beam was focused to a 200 μm spot on the sample using 350 mm focal length lens, which formed practically parallel beam on the sample. Stokes beam was focused to the same 200 μm spot on the sample plane through the microscope objective. The 50x and 100x objectives with NA 0.45 and 0.73 respectively, produced wide range of Stokes angles. While maximum Stokes angle was defined by the NA of the objective, the minimum angle was controlled by a mask that was placed on the objective and blocked the central portion of Stokes beam, which was collinear to the pump.

Initially Stokes and pump beams were counter-propagating in the sample. After passing through the sample, Stokes beam was reflected by a dichroic mirror and became co-propagating with the pump, though it had much broader angular distribution. In this illumination geometry a small-angle scattering is sufficient to get fractions of the pump and Stokes beams under phase-matching condition, necessary for efficient CARS generation.

Wide-field illumination technique requires much higher laser power in comparison to scanning methods to provide sufficient energy density over the whole field of view. We found that for 200 μm focal spot at least ~10 μJ in pump and Stokes beam is required to generate well detectable CARS signal. Regen and OPA produced pulses of the required energy at repetition rate up to 1 kHz. Pulse duration of both pump and Stokes was about 1 ps, which for CARS microscopy is proven to be optimal combination of pulse energy level and spectral width [10].

If sample is illuminated with coherent light portions of scattered, or reflected radiation may interfere with each other and produce random intensity modulated pattern – speckles – on a detector. Unlike scanning CARS, where area illuminated at any particular moment is relatively small (~1 μm) and speckles do not appear, coherent illumination of a 100 μm spot in wide-field CARS produces significant speckling. To decrease speckling we coupled Stokes beam into a 1 m long

large-core (470 μm) multimode fiber that was randomly waggled from pulse to pulse. Averaging over 100 pulses was sufficient to reduce intensity modulation caused by speckling to a few percent level.

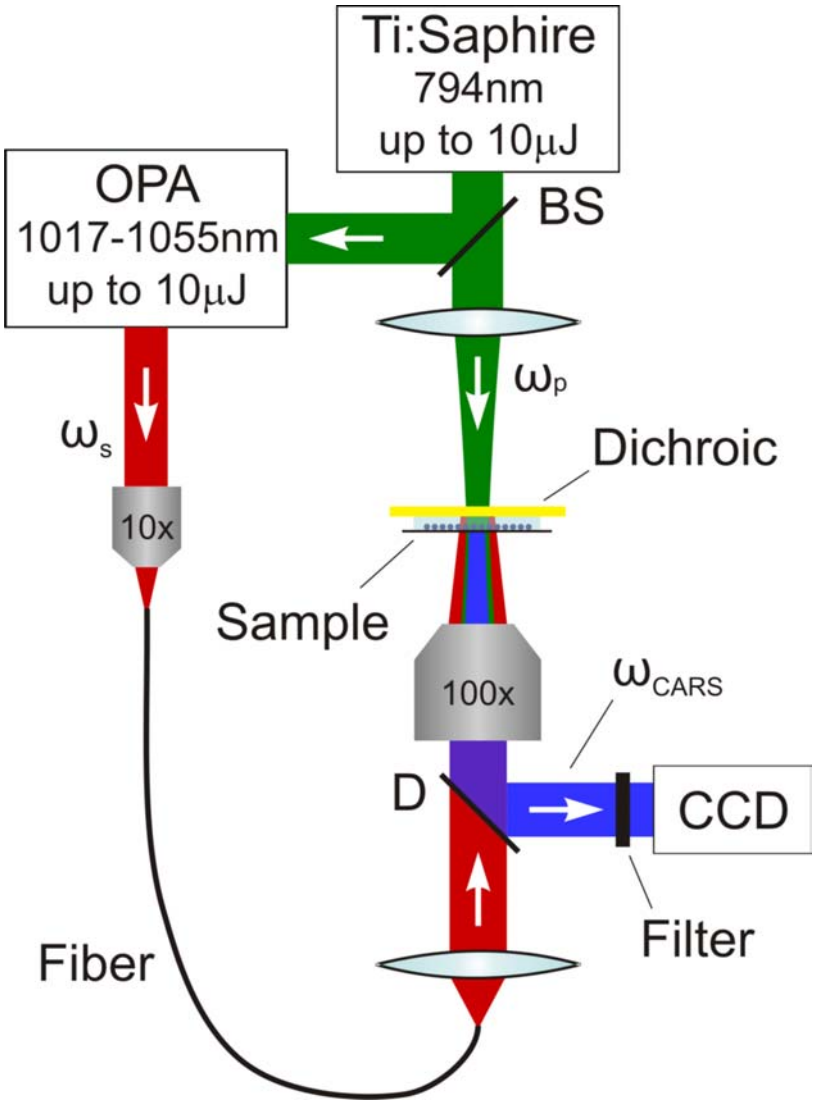

Fig. 1. Experimental setup layout. BS: 20% beam splitter, D – dichroic mirror (separates CARS from Pump and Stokes), Dichroic: dichroic mirror (reflects Stokes and transmits pump), 10x: Nikon 10x objective, NA = 0.25, 100x: Nikon 100x objective, NA = 0.73, Fiber: multimode fiber, CCD: CCD camera -Princeton Instruments LN-CCD-512

2.2 Image acquisition scheme

CARS signal was collected in forward direction (F-CARS) by the same microscope objective that was used to focus the Stokes beam. Images formed by a microscope were recorded with a liquid nitrogen cooled CCD camera (512x512 pixels) with very low dark noise (less than 1 count/min). The imaged area size was 100x100 and 200x200 μm for 100x and 50x objectives, respectively. The camera was replaced with a photomultiplier tube (PMT, Hamamatsu) for measuring total amount of signal integrated over the whole field of view. It was especially convenient for measuring power, spectral and angular dependencies of CARS, as well as for adjusting the delay between pump and Stokes beams. A dichroic mirror transparent for pump and Stokes and highly reflective for CARS wavelengths and a filter that transmitted light in a narrow range (600 – 700nm) and suppressed radiation beyond this range by more than 4 orders of magnitude was installed in front of the detector to filter out residual pump and Stokes radiation.

3. RESULTS AND DISCUSSION

3.1 Proof of principle

To demonstrate capabilities of our method it would be indicative to compare images of objects of the same shape but different chemical structure. For this purpose we used 6 μm polystyrene and quartz beads. Raman spectrum of polystyrene has sharp peak at 3070 cm^{-1} corresponding to aromatic C-H stretch vibration, while quartz does not have any pronounced features in this frequency range.

First, measurements were performed to confirm that the detected signal was produced as a result of CARS process. Using PMT we measured CARS signal dependence on pump and Stokes beams intensities. As shown in Figure 2, detected signal was found to be quadratically dependent on pump and linearly on Stokes beam intensity. Same behavior was observed for both 50x and 100x objectives and for any size (0 to 5 mm) of the mask blocking central part of Stokes beam.

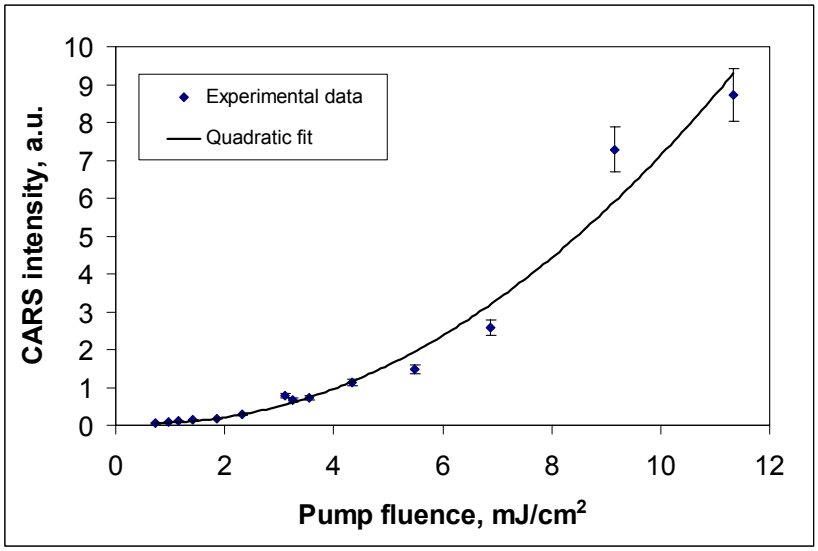

a)

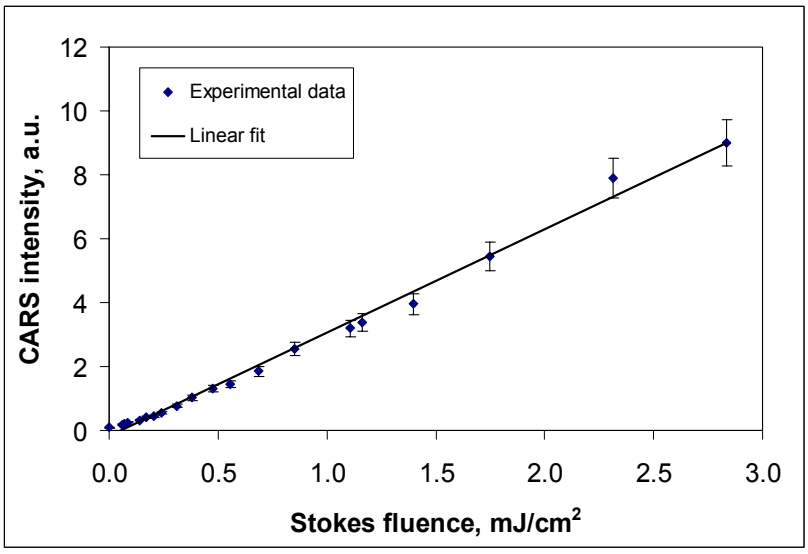

b)

Fig. 2. CARS signal from a polystyrene bead as a function of pump (a) and Stokes (b) fluences with quadratic and linear fitting curves respectively.

To choose appropriate Stokes illumination angle range we compared CARS signal obtained from a single polystyrene bead and from a 100 μm thick glass slide. As expected, without the mask strong CARS generation is observed in a glass slide. This can be explained by the fact that there is a portion of Stokes beam, which is collinear with the pump within the whole sample, and thus generates CARS signal in a homogeneous material. Increasing the mask diameter (and thereby increasing the angular size of the cut-out central part of the Stokes beam) we were able to greatly suppress CARS signal generated in the bulk material. For the blocked angle of 10^o the background was reduced by more than an order of magnitude. At the same time CARS signal produced by a polystyrene bead was reduced much less. In a first approximation this reduction can be attributed to the reduced aperture of the collecting objective. For all further measurements the angular size of the blocked area was set to 15^o.

To evaluate chemical sensitivity of the method, CARS spectrum of polystyrene beads was measured by varying the Stokes laser wavelength. For this measurement a number of polystyrene beads were deposited directly onto the dichroic mirror. In Figure 3 Raman spectrum of polystyrene [11] and measured CARS signal are shown. Distinct Raman resonance of polystyrene at 3070 cm^{-1}, is evident on both spectra.

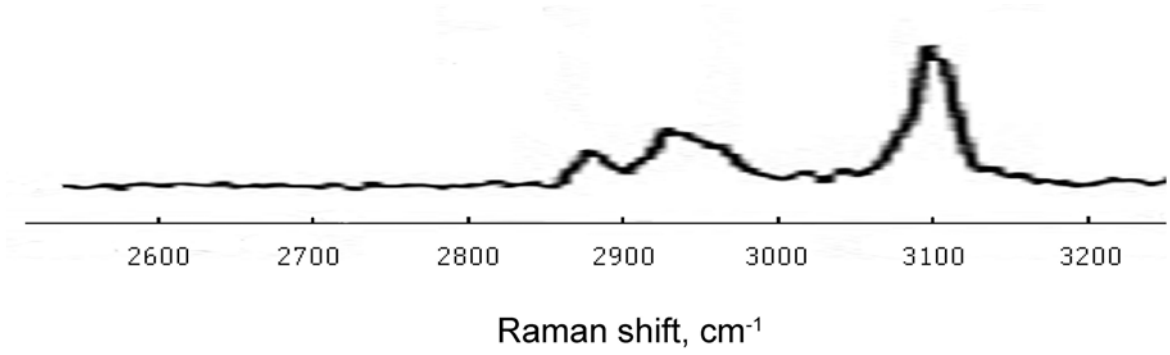

a)

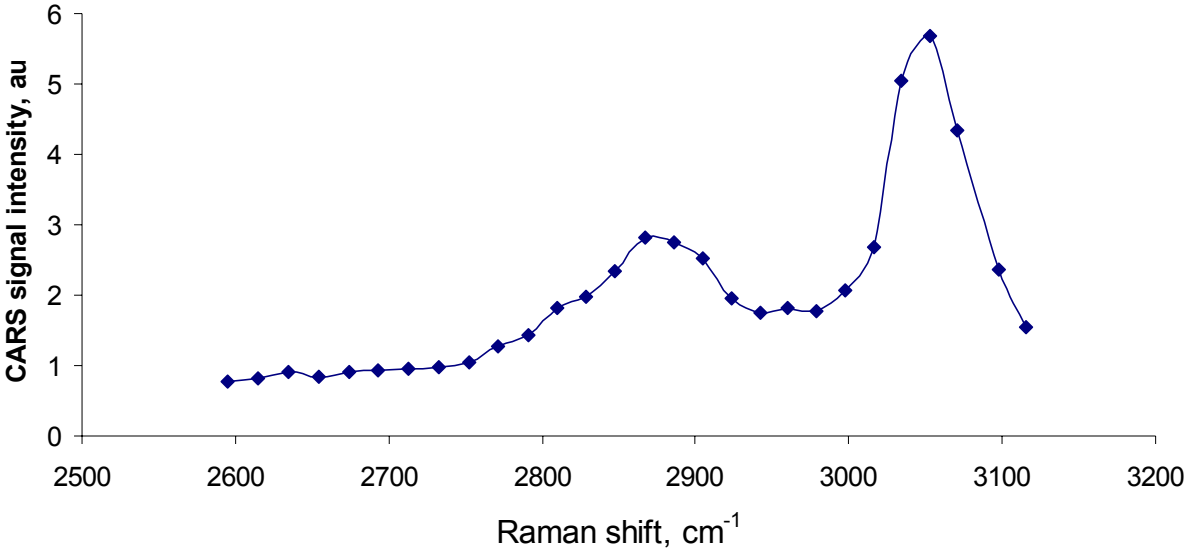

b)

Fig. 3. a) and b) Raman and CARS spectra of polystyrene respectively.

3.2 Chemically-selective imaging

To demonstrate chemically selective imaging a mixture of polystyrene and quartz beads floating in a thin (~30 μm) layer of water between the dichroic mirror and a 3 μm Mylar film was imaged at two different wavelengths: on and off the polystyrene Raman resonance. Images recorded at 3071cm^{-1} and 3116cm^{-1} are shown in Figure 4 a) and b), respectively. Intensities of the pump and Stokes beams were kept at the same levels in both cases. As expected, brightness of the quartz beads was practically the same in both cases. At the same time brightness of the polystyrene beads at resonance was considerably higher than that out of resonance. It is interesting to note that even out of the resonance polystyrene beads appeared significantly brighter than the quartz ones. One of the factors that could contribute to this effect is higher refractive index of polystyrene beads ($n_{polystyrene}$=1.59 vs. n_{quartz}=1.46). This difference in indices of the particles immersed in water (n=1.33), leads to stronger refraction of the laser beams in polystyrene beads, which is a key condition for CARS generation under non-phase matching illumination geometry.

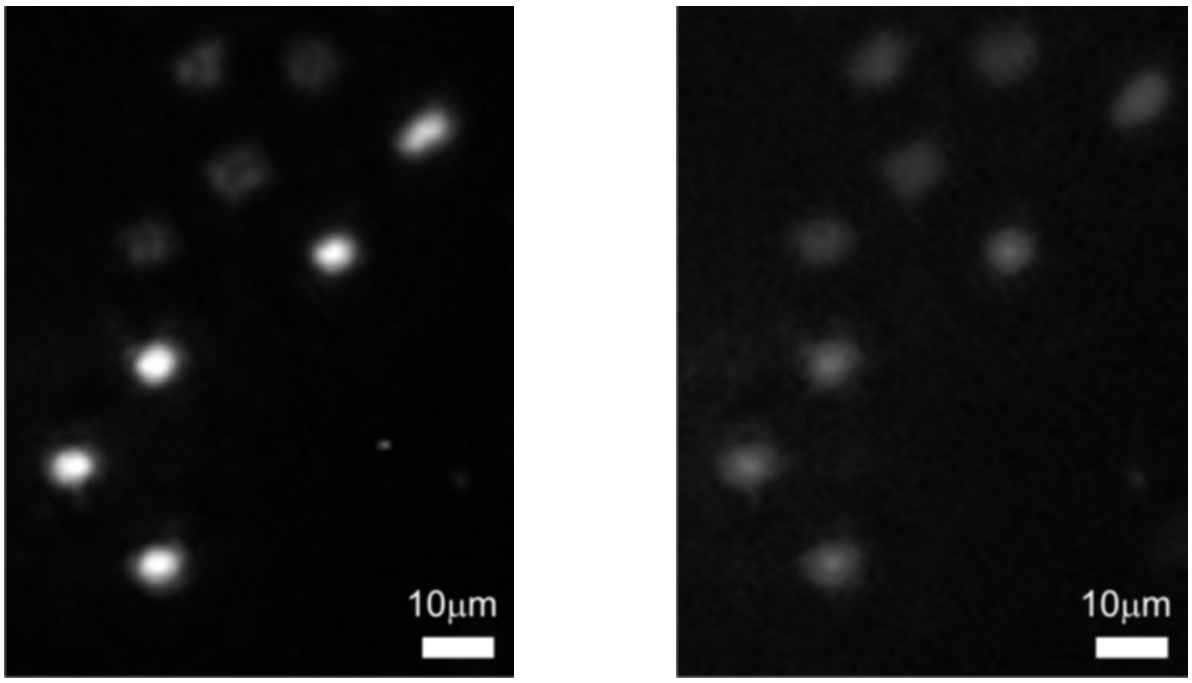

a) b)

Fig. 4. Acquired images of a mixture of polystyrene and quartz beads: a) image taken on resonance of polystyrene (Raman shift 3071 cm-1), b) image taken off-resonance of polystyrene (Raman shift 3116 cm-1).

The ratio between resonant and non-resonant CARS signal of polystyrene in water, observed in this experiment, was about 2, while dry beads have exhibited significantly higher spectral contrast of 5. This difference can be explained by the fact that in our approach scattered pump and Stokes beams can generate CARS signal not only within the scattering object, but potentially in the surrounding material as well. Apparently no such signal can be generated in the air; however in water, surrounding the sample, its contribution could be substantial. Since water doesn't have pronounced spectral features in the region of interest, signal from water will decrease the spectral contrast of the detected CARS signal.

4. CONCLUSION

We have developed and successfully tested novel non-scanning wide-filed CARS imaging technique based on non phase-matching illumination geometry that provides short image acquisition time, high spatial resolution, and chemical selectivity. The validity of the method was proven by spectral and intensity measurements and CARS images of well-defined test samples. Proposed method has potential advantages over the scanning CARS of being independent on laser fluctuations, and capable of rapid image acquisition. Single pulse imaging could be especially useful for studying rapid intracellular processes.

REFERENCES

1. R. J. H. Clark, R. E. Hester, *Advances in Non-Linear Spectroscopy*, John Wiley and Sons, New York, 1987.
2. B. S. Hudson, "New laser techniques for biophysical studies," *Ann. Rev. of Biophys. Bioengin.* 6, 135-150 (1977).
3. P. D. Maker, R. W. Terhune "Study of optical effects due to an induced polarization third order in the electric field strength," *Phys. Rev.* 137, A801-A818 (1965).
4. M. D. Duncan, J. Reintjes, T. J. Manuccia, "Scanning coherent anti-Stokes Raman microscope," *Opt. Lett.* 7, 350-352 (1982).
5. J. J. Song, G. L. Eesley, M. D. Levenson, "Background suppression in coherent Raman spectroscopy," *Appl. Phys. Lett.* 29(9), 567-569 (1976).
6. J.-X. Cheng, A. Volkmer, L. D. Book, X. S. Xie, "An epi-detected coherent anti-Stokes Raman scattering (E-CARS) microscope with high spectral resolution and high sensitivity," *J. Phys. Chem. B,* 105(7), 1277-1280 (2001).
7. M. Mueller, J. Squier, C. A. de Lange, G. J. Brakenhoff, "CARS microscopy with folded BoxCARS phasematching," *Journal of Microscopy* 197(2), 150-158 (2000).
8. A. Zumbusch, G. R. Holton, X. S. Xie, "Three-dimensional vibrational imaging by coherent anti-Stokes Raman scattering, " *Phys. Rev. Lett.* 82, 4142-4145 (1999).
9. C. Heinrich, C. Meusburger, S. Bernet, M. Ritsch-Marte, "CARS microscopy in a wide-field geometry with nanosecond pulses," *Journal of Raman Spectroscopy* 37, 675-679 (2006).
10. J.-X. Cheng, X. S. Xie, "Coherent anti-Stokes Raman scattering microscopy: instrumentation, theory, and applications," *J. Phys. Chem. B* 108, 827-840 (2004).
11. R. L. McCreery, http://www.chemistry.ohio-state.edu/~rmccreer/freqcorr/images/poly.html